Journal of Materials Chemistry C

ROYAL SOCIETY OF CHEMISTRY

PAPER

View Article Online
View Journal | View Issue

Cite this: J. Mater. Chem. C, 2024, 12, 12906

Precise molecular design for a twisted pyrene-thiophene based mechanofluorochromic probe with large Stokes shift and feasibility study towards security ink and re-writable papers†

Ram Prasad Bhatta,[a] Sumit,[a] Vishal Kachwal,[a] Vandana Vishwakarma,[b] Angshuman Roy Choudhury[b] and Inamur Rahaman Laskar *[a]

The creation of MFC-active smart molecules by tuning functionality has received considerable attention owing to its versatile applicability. Pyrene-based twisted donor–acceptor (D–A) dyes (**PySS** and **PySP**) have been synthesized and characterized. Here, the pyrene is directly connected with thiophene, and this unit is further linked terminally to photoactive species (thiophene/pyridine) *via* a four-carbon unit conjugated spacer. These molecules show excellent solvatochromic properties, with a substantial shifting of the emission wavelength (**PySS**- 147 nm and **PySP**- 130 nm). The lowest transition state contains a significant contribution from ICT characteristics, as evidenced by spectral analysis and computational calculations. Moreover, these are identified as 'aggregation-induced enhanced emission' (AIEE) active compounds and exhibit mechanofluorochromism (MFC). By grinding, **PySS** and **PySP** display MFC features with 50 nm and 54 nm red shifting, respectively. Interestingly, **PySS** shows a gradual emission change from green (510 nm) to orange emission (578 nm) by gradually changing the pressure with a hydraulic press (0 to 12.5 tons). The single crystal structure of both compounds was investigated to understand the structure–property relationship for MFC. The crystal packing shows that the twisted molecules (dihedral angle between pyrene and thiophene is 59.36° and 56.93° for **PySS** and **PySP**, respectively) are loosely bound with several weak interactions (C–H···π, C–π···H, H···H, C–H···O). Interestingly, it was observed that two molecules in a unit cell are arranged in an antiparallel fashion; these molecular pairs are linearly connected to another pair axially, forming a long one-dimensional chain-type arrangement. On applying pressure, these twisted molecular pairs may slowly planarize, leading the molecules to come closer, thus changing the molecular interaction and the emission properties. A feasibility study of the potentiality of using these compounds in data encryption–decryption and security ink has also been demonstrated.

Received 2nd June 2024,
Accepted 8th July 2024

DOI: 10.1039/d4tc02262a

rsc.li/materials-c

Introduction

Mechanofluorochromic (MFC) materials are a class of smart stimuli-responsive materials in which the emission properties of the material change upon the application of stress.[1] Organic mechanofluorochromic (MFC) materials (that change their emission under anisotropic and isotropic pressure) have attracted great attention in recent years due to their promising applications in sensing pressure, storage devices, security inks, three-dimensional (3D) printing, *etc.*[2–5] Stimuli-responsive materials with tunable emission and reversible switching are highly demanding for different applications, such as security encryption devices, deformation detectors, fluorescent probes, switches, and optoelectronic devices.[6,7] The process of protein folding and unfolding, as well as the movement of cells, can be influenced by pressure in biology.[8] Due to the influence of the aggregation-caused quenching (ACQ) effect, most of the conventional organic chromophores exhibit weakened or even totally quenched emission in the aggregated state, which limits the development and application of MFC materials to a greater

[a] Department of Chemistry, Birla Institute of Technology and Science (BITS), Pilani Campus, Pilani, Rajasthan 333031, India. E-mail: ir_laskar@pilani.bits-pilani.ac.in
[b] Department of Chemical Sciences, Indian Institute of Science Education and Research (IISER), Mohali, Sector 81, S. A. S. Nagar, Manauli PO, Mohali, Punjab 140306, India

† Electronic supplementary information (ESI) available. CCDC 2349027 and 2349045. For ESI and crystallographic data in CIF or other electronic format see DOI: https://doi.org/10.1039/d4tc02262a

extent.[9,10] A new opportunity to overcome the ACQ problem and develop durable solid-state luminescent materials is presented through the generation of 'aggregation-induced emission' (AIE) compounds.[11] Compounds with AIE properties usually possess a twisted geometry. Stimuli-responsive organic materials with AIE characteristics would be an interesting platform to explore the structure–property relationship for future designing MFC compounds.

In several reports, it has been observed that AIE active organic compounds exhibit distinct responses in emission properties upon mechanical grinding (anisotropic) and hydrostatic pressure (isotropic).[1] The isotropic force is applied uniformly by the diamond anvil cell (DAC). The mechanochromic luminescence performance of AIEgens can be explained as a synergetic process associated with the changing of the molecular conformations, the molecular packing forms and weak intermolecular interactions (such as C–H···π, C–H···O, and C–H···N hydrogen bonds).[6,12,13] The majority of mechanochromic luminescent materials have loose and metastable packing, and are believed to be critical factors in achieving structural transformation and pressure-dependent multicolor emissions. After grinding or compressing physically, these weak intermolecular interactions are altered, resulting in the variation of the stacking mode and the molecular conformation, and finally causing the emission color change.[14–16]

In 2012, Tian *et al.*[17] reported mechanochromic luminescence of a 9,10-distyrylanthracene (DSA) derivative 9,10-bis[(*E*)-2-(pyridin-2-yl)vinyl]anthracene (BP2VA). This molecule showed extraordinary luminescence properties: grinding and applying external pressure changed the photoluminescence (PL) of the BP2VA powder from green to red color. With the external pressure increasing from 0 to 8 GPa, the emission of BP2VA powder showed a gradual red shift from green to red distinctly. There are many reports found from carbon nanodots, metal–organic frameworks (MOFs), covalent organic frameworks (COFs), *etc.* which enriched the chemistry of MFC materials.[18–23] The majority of high-contrast solid-state MFC materials include tetraphenyl ethylene (TPE),[24–26] triphenylamine (TPA),[27–29] anthracene,[30–32] carbazole, phenothiazine, stilbene, spiropyrans, *etc.*[33–39] Pyrene is a highly planar and conjugated molecule. Hence, it is prone to form a dimer structure due to strong π–π stacking during the aggregation process.[40,41] In 2020, Xiong *et al.*[13] synthesized (4-(phenothiazin-10-yl)phenyl)(pyren-1-yl)-methanone (Py-BP-PTZ) which exhibits AIEE, polymorphism and mechanochromic properties. It shows gradually red shifted emission under high pressure by DAC, and the planar pyrene derivative changes emission mainly due to planarization under high pressure and change of the molecular packing mode with changing intermolecular interactions. Very recently (2024), Eldhose *et al.*[42] reported an MFC property of AIE active pyrene-based compounds and investigated the molecular packing and explained the role of molecular interaction for luminescence behavior. Pyrene-based molecules are enriched in optical properties because of a highly electron-rich polyaromatic system. Some of the pyrene-based materials with high contrast solid-state emission are reported for MFC properties, but there still remain many challenges in terms of controllable approaches to yield high-quality pyrene-based protocols, morphological modulation, unclear structure–function relationships, *etc.*[43,44] The pyrene derivatives reported to date show some degree of fluorescent quenching in the solid state.[45,46] Developing pyrene-based fluorescent molecules with good solid-state emission properties is still a challenge.

In 2017, our group (Pasha *et al.*) reported an AIE active salicylaldehyde-based Schiff base that exhibited a reversible change of emission color gradually with applying pressure slowly.[47] The reported molecule (shown below) has twisted D–A-type features with ICT characteristics.

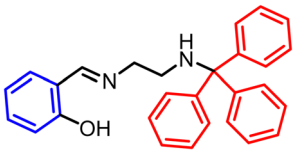

After analyzing the packing of the crystal structure, it was found that two molecules form a pair aligned in an opposite manner with a definite weak interaction across the two molecules. Each of the pairs is connected axially forming a long linear chain and these chains are connected horizontally through intermolecular interactions resulting in a molecular sheet. To determine the molecular structure that is responsible for demonstrating a particular way of molecular arrangement described above, more study is required with consideration of the appropriate molecular structure.

Recently, a pyrene and acyl-thiophene connected D–A type molecule [1-(5-(pyren-1-yl)thiophen-2-yl)ethan-1-one (PySY)] has been synthesized[48] and the dihedral angle was observed to be ∼48° (pyrene and thiophene plane). The compound was found to be sensitive to shearing force (by grinding) with hypsochromic emission shifting (yellow to green). But it does not respond to mechanofluorochromism with applying pressure (compressive force). To make the present compound sensitive towards pressure imposed mechanofluorochromism, mimicking our previous work,[48] a four-unit conjugated spacer attached to the thiophene side (of the pyridine-acyl substituted thiophene) along with some photoactive species connected terminally. Here, two compounds (**PySS** and **PySP**, shown below) have been synthesized, their MFC properties (shearing and compressive forces) were studied, and the feasibility study towards data encryption–decryption and security inks was checked.

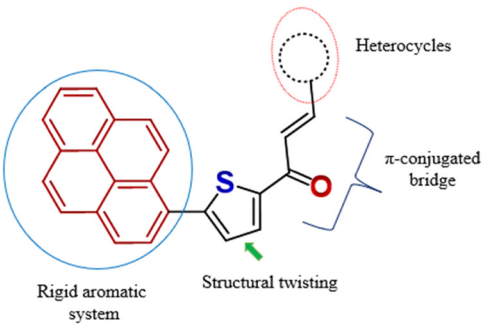

Experimental section

Materials

We purchased 1-bromopyrene, palladium(0), thiophene-2-aldehyde and pyridine-2-aldehyde from TCI chemicals. 5-Acetyl thiophene-2-boronic acid was bought from Alfa Aesar. Inorganic salts such as sodium carbonate, potassium carbonate, sodium hydroxide, and potassium hydroxide, *etc.* were obtained from Merck, and UV-graded solvents like tetrahydrofuran (THF), hexane, cyclohexane, carbon tetrachloride (CCl_4), toluene, acetone, *N*,*N*-dimethylformamide (DMF), dimethyl sulfoxide (DMSO), dichloromethane (DCM), ethanol and methanol were purchased from the Spectrochem company. All these chemicals were used without any further purification.

Measurement and characterization

^{1}H NMR and ^{13}C NMR spectra were recorded using a 400 MHz Bruker NMR spectroscope. High-resolution mass spectra (HRMS) were recorded on an Agilent Q-TOF LC-MS spectrometer in positive electrospray ionization (ESI) mode. UV-VIS absorption spectra were recorded using a Shimadzu spectrophotometer (models UV-1800 and 2550), and solid-state UV-VIS absorption spectra were recorded by a Shimadzu UV-2450, UV-VIS spectrophotometer in absorption mode. Steady-state photoluminescence (PL) spectra were recorded on a Horiba Jobin Yvon spectrofluorometer (FluoroMax-4 and Horiba 'Fluoro Log' Spectrofluorometer). Powder X-ray analysis was performed using a Rigaku Mini-Flex II diffractometer with incident Cu-Kα (λ = 1.54 Å) radiation. Raman analysis was performed by using a HORIBA, AIST-NT (Model: Labram HR Evolution, Omega Scope). The quantum yields of the compounds were obtained on a Quanta-Phi (F-3029) accessory connected to the Fluoro-Max-4. The lifetime of the compounds was recorded on a Horiba Delta Flex 01. Thermogravimetric analysis (TGA) was performed by TGA-50, SHIMADZU equipment at 10 °C min^{-1}, under a nitrogen atmosphere. A differential scanning calorimetry (DSC) study was performed by using a DSC-60 plus instrument from SHIMADZU equipment at 10 °C min^{-1}, under a nitrogen atmosphere. A model- "Apreo LoVac" FE-SEM was used to investigate the morphology of all forms of isolated compounds.Single crystal X-ray diffraction data was collected on Rigaku XtaLABmini X-ray diffractometer equipped with Mercury CCD detector, graphite monochromatic Mo-Kα radiation (λ = 0.71073 Å) at 100.0 (2) K using ω scans (see supporting documents for details).

Synthesis of PySS and PySP

The synthetic scheme of the pyrene thiophene-based compounds (**PySS** and **PySP**) is summarized below (Scheme 1).

Initially, the compound 1-(5-(pyren-1-yl)thiazol-2-yl)ethan-1-one (**PyS**) was synthesized by following an earlier method reported by our group.[48] To synthesize **PySS**, **PyS** (0.3 gm, 0.92 mmol) in ethanol (4 ml) was stirred for 30 min at 50 °C and cooled to (10–15) °C, then to the clear solution of reaction mass, NaOH (10% aq. solution, 1 ml) was added slowly and the

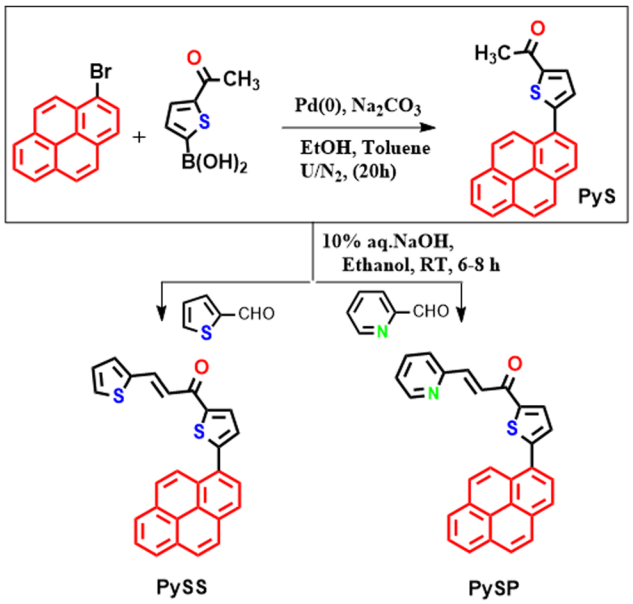

Scheme 1 Synthetic route for the compounds (**PySS** and **PySP**).

reaction mixture was further stirred for 10–15 min followed by adding thiophene-2-aldehyde (0.155 gm, 1.38 mmol). Then, the reaction mass was stirred for 10–12 h at 40–50 °C. The reaction mass temperature was slowly cooled to RT, then water (3.0 ml) was added which resulted in precipitate formation, and the reaction mass was filtered, washed with chilled ethanol, and the obtained product was dried for 12 h under vacuum. A dried product (350 mg, 90% yield) was obtained. A similar process was followed to synthesize **PySP**. The synthesized compounds were characterized by NMR and HRMS (Fig. S1–S9, ESI†).

PyS (1-(5-(pyren-1-yl)thiazol-2-yl)ethan-1-one)

^{1}H NMR (400 MHz, chloroform-*d*) δ/ppm: 8.4696–8.4928 (d, 1H, J = 9.28 Hz), 8.2745–8.2228 (m, 3H), 8.1776–8.1275 (m, 3H), 8.1078–8.0567 (m, 2H), 7.8692–7.8596 (d, 1H, J = 3.84 Hz), 7.4373–7.4277 (d, 1H, J = 3.84 Hz), 2.6862 (s, 3H). ^{13}C NMR (100 MHz, chloroform-*d*) δ/ppm: 190.72, 151.54, 132.72, 131.77, 131.43, 130.85, 128.97, 128.91, 128.52, 128.37, 128.08, 127.28, 126.35, 125.76, 125.43, 124.65, 124.36, 26.74. LC-HRMS (ESI): found *m*/*z*: 327.0837 [M + H]$^+$. Calculated *m*/*z*: 326.0835.

PySS ((*E*)-1-(5-(pyren-1-yl)thiophen-2-yl)-3-(thiophen-2-yl)prop-2-en-1-one)

^{1}H NMR (400 MHz, chloroform-*d*) δ 8.52 (d, J = 9.3 Hz, 1H), 8.25 (td, J = 7.9, 2.7 Hz, 3H), 8.15 (dd, J = 9.7, 7.2, 2.9 Hz, 4H), 8.12–8.03 (m, 2H), 8.01 (d, J = 3.9 Hz, 1H), 7.48 (dd, J = 4.4, 2.1 Hz, 2H), 7.43 (d, J = 3.6 Hz, 1H), 7.34 (d, J = 15.3 Hz, 1H), 7.15 (dd, J = 5.0, 3.6 Hz, 1H). ^{13}C NMR (100 MHz, chloroform-*d*) δ/ppm: 181.44, 151.61, 145.67, 140.28, 136.28, 132,19, 132.08, 131.74, 131.41, 130.84, 129.09, 128.91, 128.88, 128.58, 128.54, 128.42, 128.37, 128.13, 127.29, 126.35, 125.76, 125.43, 125.01, 124.69, 124.64, 124.42, 120.33. LC-HRMS (ESI): found *m*/*z*: 421.0715 [M + H]$^+$, calculated *m*/*z*: 420.0643.

PySP (*E*)-1-(5-(pyren-1-yl)thiophen-2-yl)-3-(pyridin-2-yl)prop-2-en-1-one

^{1}H NMR (400 MHz, chloroform-*d*) δ 8.75 (dt, J = 4.6, 1.5 Hz, 1H), 8.54 (d, J = 9.3 Hz, 1H), 8.29–8.21 (m, 3H), 8.20–8.10 (m, 5H), 8.13–8.03 (m, 2H), 7.90 (d, J = 15.1 Hz, 1H), 7.79 (td, J = 7.7, 1.8 Hz, 1H), 7.57–7.51 (m, 1H), 7.50 (d, J = 3.8 Hz, 1H), 7.35 (ddd, J = 7.6, 4.7, 1.2 Hz, 1H). ^{13}C NMR (101 MHz, chloroform-*d*) δ 182.13, 153.12, 152.26, 150.24, 145.72, 142.02, 136.98, 132.98, 131.79, 131.42, 130.85, 129.21, 128.91, 128.59, 128.57, 128.41, 128.16, 127.31, 126.38, 125.80, 125.76, 125.48, 125.16, 125.03, 124.73, 124.66, 124.52, 124.44. LC-HRMS (ESI): found m/z: 416.1131 $[M + H]^+$, calculated m/z: 415.1031.

Preparation of AIEE solution

An "aggregation-induced emission enhancement" (AIEE) study of the prepared probe molecules (**PySS** and **PySP**) was performed. A stock solution of compounds (10^{-4} M in THF) was prepared first and then 0.5 ml of each probe solution was taken in a glass vial of 5 ml volume. For preparing the 0% water fraction, 4.5 ml of THF, for the 20% water fraction, 1.0 ml water and 3.5 ml THF, for the 40% water fraction, 2.0 ml of water and 2.5 ml THF, for the 60% water fraction, 3.0 ml water and 1.5 ml THF, and for the 90% water fraction, 4.5 ml water was added. The total volume was made to 5 ml for all the vials.

Computational studies

The DFT-based computational calculations were performed by the Gaussian 16 package,[49–51] using the ωB97X-D exchange–correlation functional.[52] The 6-311+G(d,p) basis set was employed to consider polarization and diffusion effects in the molecules. All the computational study was done in a gaseous state. The optimized structure with the HOMO–LUMO distribution is shown in Fig. 2.

Results and discussion

Synthesis of solid-sate emitters

The synthetic scheme of pyrene thiophene-based compounds is summarized in Scheme 1. Initially, **PyS** was synthesized by using the earlier reported method of our group.[48] **PySS** and **PySP** were synthesized using the Claisen–Schmidt condensation reaction between **PyS** and the corresponding aldehyde (Scheme 1). The synthesized compound was characterized by NMR and HRMS (Fig. S1–S9, ESI†). The molecular structure of both compounds was determined by single-crystal X-ray diffraction studies (Fig. 3). Thermogravimetric analysis (TGA) of the molecules shows that these molecules are stable up to 320 °C (Fig. S26, ESI†).

Photophysical properties

The UV-VIS absorption spectra of the synthesized compounds (**PySS** and **PySP**) were recorded in THF (10 μM) solution. It shows absorption peaks at two major regions, intense and sharp peaks observed at ~230–260 nm and broad vibronic peaks at ~300–400 nm (Fig. 1). The intense absorption peak at 242 nm corresponds to the $^1\pi$–π^* transition of pyrene moieties in both compounds.[48] The absorption band in the long-wavelength region (300–400 nm) can be attributed to a mixed $^3\pi$–π^* transition with a charge transfer (CT) character that belongs to the push–pull chalcone π-system.[53–56] Solid state absorption of **PySS** and **PySP** was recorded; **PySS** shows a broad and red-shifted absorption tailing up to 600 nm and similarly, for the **PySP** case, absorption tailing up to 560 nm (Fig. S10, ESI†). The emission spectra of the powder sample of both compounds were recorded at excitation, λ_{max} = 400 nm, and the emission peak was observed at 510 nm for **PySS** and 531 nm for **PySP** (Fig. S10, ESI†). In the dilute solution of THF (10^{-4} M), emission maxima were observed at 509 nm and 520 nm for **PySS** and **PySP**, respectively (Fig. 1).

The solvatochromic properties of **PySS** and **PySP** were investigated with UV-VIS absorption and photoluminescence (PL) spectroscopy in solvents with varying polarities (Fig. S11 and S12, ESI†), and the corresponding data are summarized in Tables S1 and S2 (ESI†). It was observed that with increasing polarity of the solvent, continuous red-shifting of the emission band occurs (Fig. S11 and S12, ESI†). To better understand the solvatochromic behavior, the relationship between the solvent polarity parameter (Δf) and the Stokes' shift ($\Delta\nu$) based on the

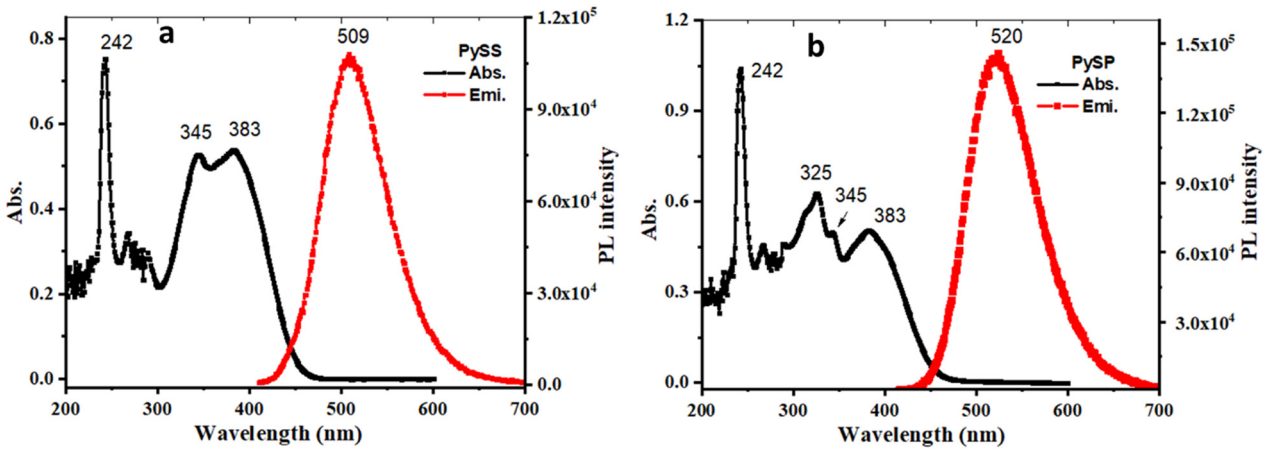

Fig. 1 Absorption spectra (black line) with 10 μM concentration and emission (red line) with a concentration of 100 μM of **PySS** (a) and **PySP** (b) in THF.

Lippert–Mataga equation was investigated. As shown in (Fig. S13a, ESI†), **PySS** displays a linear dependence of $\Delta\nu$ on Δf, which suggests that solvents with strong polarity are able to stabilize the excited state *via* the reorientation of the solvent molecules,[57] resulting in a lowered energy of the system and the bathochromically shifted emission maximum. In the case of **PySP** (Fig. S13b, ESI†), relatively more deviation was observed from the linearity. The protic polar solvent (MeOH) deviates more because of the presence of a pyridine ring, and the nitrogen possibly forms a hydrogen bond with MeOH. From the literature, we found that solvatochromic properties were observed mainly because of the ICT (intramolecular charge transfer) and TICT (twisted intramolecular charge transfer) character of the molecules.[55] Here, we observed that **PySS** and **PySP** are highly sensitive towards the solvent polarity, for **PySS** ~ 147 nm shifting from hexane to methanol and in the case of **PySP** ~ 130 nm red shift from hexane to DMSO (Fig. S11 and S12, ESI†). The formation of an excimer and intramolecular charge transfer (ICT) are two possibilities that can account for the emission changes. Pyrene has a rigid planar system; it tends to form an excimer at high concentrations.[58,59] The packing diagram of **PySS** (Fig. 7) clearly shows the absence of any pyrene–pyrene interaction, thus excluding the possibility of the formation of any excimer. However, the packing diagram of **PySP** (Fig. 8) shows the weak pyrene–pyrene interaction, which indicates the possibility of the formation of an excimer. To examine whether an excimer was formed in this system, the PL spectra of **PySP** in DCM solution with increasing concentrations (10^{-2} to 10^{-6} M) were recorded (Fig. S14, ESI†). However, no clear peak shifting was observed, indicating that no excimer was formed. Therefore, it is speculated that the lowest emitting state consists of ICT characters for **PySS** and **PySP**. To verify this fact, computational calculations of pyrene thiophene in its optimized lowest energy gas phase were performed using the Gaussian 16 package. The frontier orbital plots of the HOMO and LUMO are shown in Fig. 2. The HOMO of **PySS** was mainly distributed on pyrene and immediately connected to the thiophene moiety, whereas the LUMO of **PySS** was majorly shifted towards the second thiophene through the π-electron bridge. In the case of **PySP**, it was observed that the HOMO is located on the pyrene and immediately connected to the thiophene and the LUMO is located on the pyridine-carbonyl side of the molecule. Since the distributions of the HOMO and LUMO were separated in the donor–acceptor system, this emission will be consistent with the proposed ICT character.

It was observed from the optimized structure of both the molecules that the dihedral angle between the pyrene and attached thiophene is in the range of 50–52°. The observed twisted structure hints at the possibility of 'Aggregation-induced Emission Enhanced' (AIEE) behaviour of **PySS** and **PySP**. To check the AIEE behavior, a 100 μM tetrahydrofuran solution of **PySS** and **PySP** was prepared as a stock solution. Then, AIEE solutions were prepared by varying the water fraction (v/v%) from 0% to 90% (details given in the Experimental section). In the case of **PySS** (Fig. S15, ESI†), the PL intensity slightly decreases with redshifted emission observed until 60% water fraction (f_w), and then a sudden rise of PL intensity was observed. In the case of **PySP** (Fig. S16, ESI†), the PL intensity decreases up to 40% water and then slightly increases up to 70% water fraction, and then a sharp increment is observed. The extended molecular conjugations for exciton movements are responsible for the redshifted emission upon aggregation.[60,61] From the single crystal analysis (Fig. 7 and 8), **PySS** and **PySP** have many intermolecular interactions and short contacts (Table S4, ESI†) between the neighbouring molecules. These contacts will be involved in restricting rotational motion, facilitating the excited state molecules to be relaxed in a radiative pathway.

Single-crystal X-ray structures were investigated to comprehend solid-state AIEE, and MFC behavior for these fluorophores. Single crystal structures of **PySS** and **PySP** were grown in the DCM/Hexane system by a slow diffusion process

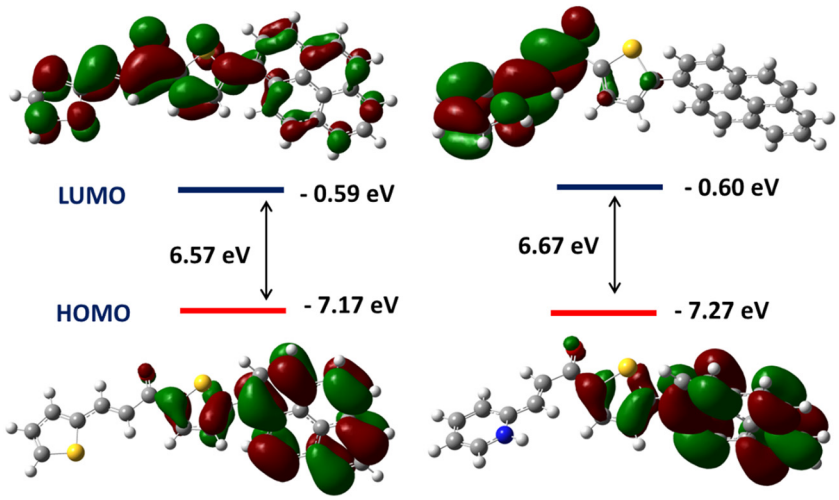

Fig. 2 The spatial electron distributions of the HOMOs and LUMOs of **PySS** (left) and **PySP** (right), which were calculated using the ωB97X-D/6-311++G(d,P) level by the Gaussian 16 package.

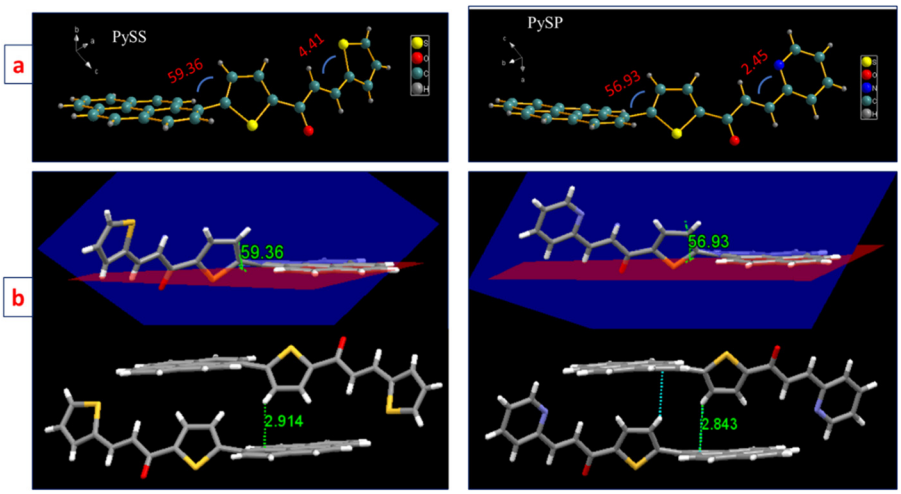

Fig. 3 (a) The asymmetric unit of **PySS** and **PySP** with dihedral angles. (b) The angle between the thiophene plane and the pyrene plane is more than 55° in both cases. The unit cell contains two molecules that are lying in antiparallel orientation. Two molecules interacted through C–H···π interactions (**PySS**-2.914 Å and for **PySP** two identical short contacts of 2.843 Å).

(CCDC- for **PySS**- 2349027 and **PySP**- 2349045†). In the crystal structure of **PySS**, pyrene and thiophene are in different planes having a dihedral angle of 59.36°, and the unit cell consists of two molecules facing opposite to each other (see left side of Fig. 3). Similarly, in the case of **PySP**, the pyrene and thiophene planes are different with a dihedral angle of 56.93°, and unit cell molecules are facing opposite to each other (right side of Fig. 3). The angle between the plane of two thiophene rings in the case of **PySS** is at 23.54° and the plane of the thiophene and pyridine rings in the case of **PySP** is at 20.45°.

Mechanofluorochromic properties of PySS and PySP

Initially, the solid-state emission properties of both compounds were recorded in powder form. Interestingly, both molecules were emissive in the solid state with a reasonably high quantum yield: compound {λ_{max}, absolute quantum yield (% Φ_f)}: **PySS** (510 nm, 24.13); **PySP** (531 nm, 19.01). The MFC features of these molecules were studied by grinding (using a mortar pestle) and by applying compressive force (using hydraulic pallet press). After grinding, **PySS** and **PySP** show large bathochromic emission shifts. It was observed that for the case of **PySS**, the emission shifted 50 nm from green to yellow (Fig. 4a), and for the case of **PySP**, the emission shifted 54 nm from greenish yellow to orange emission (Fig. 5a). The reversibility of ground samples of **PySS** and **PySP** was checked without giving any stimuli at ambient temperature. The original emission of both the compounds returned within 1 h. As no external stimuli were required to bring these to their original state, the compounds can be used as self-reversible MFC materials.[62]

Interestingly, the MFC behavior of **PySS** and **PySP** was reversible on fumigation with methanol vapor/heating at 70–80 °C for 1–2 min, and the same platform can be reused

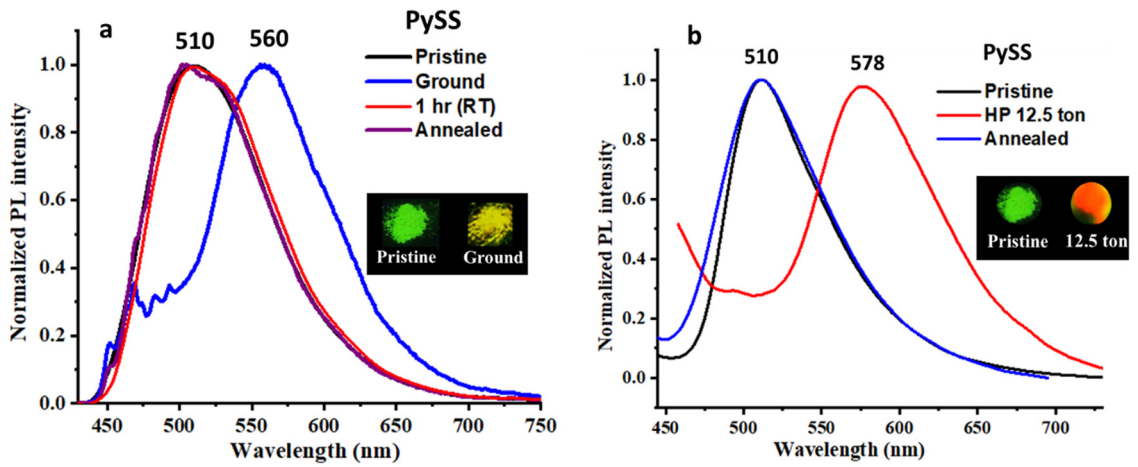

Fig. 4 (a) PL spectra of **PySS** in the pristine form and after grinding with the help of a mortar and pestle; 1 h (RT) indicates that the ground sample was kept for 1 h at rt and then the emission was recorded. (b) PL spectra of **PySS** after applying hydraulic press (HP) of 12.5 ton and heating at 70–80 °C for 1–2 minutes (annealed sample).

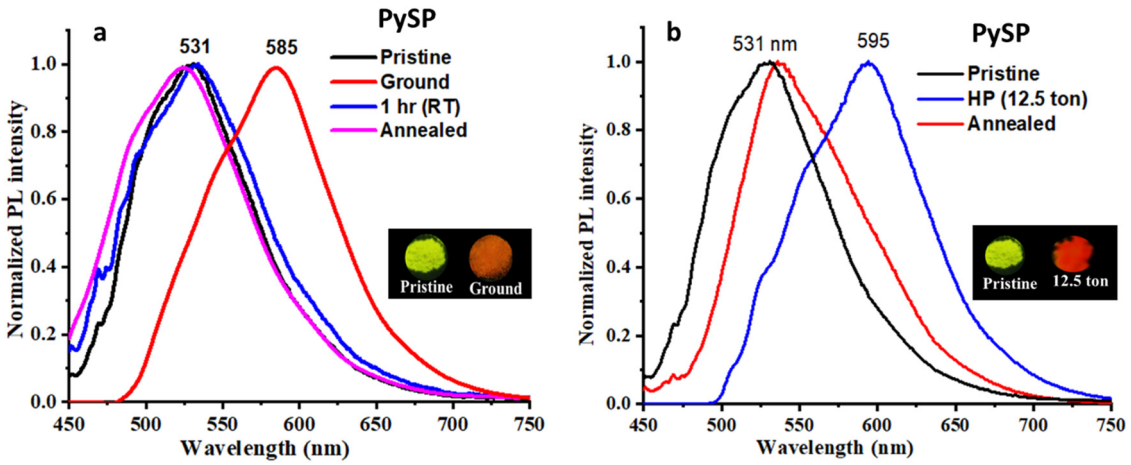

Fig. 5 (a) PL spectra of **PySP** in the pristine form and after grinding with the help of a mortar and pestle. 1 h (RT) indicates that the ground sample was kept for 1 h at RT and the emission was recorded. (b) PL spectra of **PySP** after applying hydraulic press (HP) of 12.5 ton and heating at 70–80 °C for 1–2 min (annealed sample).

more than five times (Fig. S17 and S18, ESI†). These compounds are highly sensitive to a shearing force, and a clear change of emission could be observed by simply rubbing with a metal spatula (Fig. S29, ESI†). Another efficient feature of **PySS** and **PySP** is their responsiveness towards hydraulic pressure (compressive force). Pristine samples of **PySS** and **PySP**, after applying hydraulic pressure of 12.5 tons, showed an increment of the bathochromically shifted emission of 68 nm (**PySS** case Fig. 4b) and 64 nm (**PySP** case, Fig. 5b), respectively.

On slowly changing the pressure with a hydraulic press from 0 to 12.5 tons, the original green emission of **PySS** is gradually transformed through variable intermediate emission colors (yellow, yellow-orange, orange) and finally changed to orange red (λ_{max} = 510 nm → 578 nm). It slowly reverts into the pristine form after releasing pressure within 24 h at ambient conditions and returns within 2–3 min with heating at 60–70 °C (Fig. 6). We have shown the images to describe the recovery process with heating (Fig. S30a, ESI†) and without any external trigger (Fig. S30b, ESI†). It was observed that with gradually increasing pressure (0 to 12.5 tons applied for 2 min each), the emission wavelength increases continuously (Fig. 6c). The solid-state UV-VIS absorption spectra were recorded at different pressures (0 to 12.5 tons) and it was observed that by increasing the pressure, the absorption at ∼445 nm gradually decreased along with the observation of a new redshifted peak at ∼505 nm (Fig. S19, ESI†).

This observation hints that the pyrene-attached twisted thiophene ring (supported by SXRD) becomes planar with the pyrene plane, facilitating the approaching of molecules with each other under compression, thus decreasing intermolecular distances and hence increasing interactions.[63] The lifetime study and absolute quantum yield measurement of the pristine sample, ground sample, and compressed (12.5 tons) sample were recorded for **PySS** and **PySP** (Table S3, ESI†). It was found that the excited state lifetime increases after mechanical grinding and compressive force for both compounds (Fig. S20, ESI†). The quantum efficiency (QY) of both compounds is increased after grinding, while the QY decreases after pressing (12.5 tons) (Table S3, ESI†). The powder XRD diffractograms of the pristine powder of **PySS** and **PySP** exhibited many sharp and strong scattered peaks, supporting good crystallinity with ordered molecular packing (Fig. S21, ESI†). However, the ground powder showed less intensity with some of the peaks disappearing implying their less crystalline or semi-crystalline nature. From the DSC, **PySS** shows the melting point at 190.5 °C and 191.5 °C for the pristine and ground phases, respectively (Fig. S23, ESI†). Similarly, **PySP** shows a melting temperature at 207.9 °C and 208.7 °C (Fig. S24, ESI†), for the pristine and ground samples, respectively. After having DSC data of the ground form of both compounds, we did not observe any phase transition which might be because of the highly reversible nature of the ground form of the compounds. The melting point of both compounds was recorded, and the melting range is 188–192 °C for **PySS** and 207–210 °C for **PySP**. The compounds (**PySS** and **PySP**) were filled in melting capillaries and the emission was captured before and after melting under UV (365 nm) excitation (Fig. S25, ESI†). After melting, the bathochromic emission shifting for both compounds was observed, which supports the phase transition results in bathochromic emission shifting.[39] TGA analysis of **PySS** and **PySP** showed that both compounds are thermally stable up to ∼320 °C (Fig. S26, ESI†). As already discussed in photophysical properties, the synthesized molecules show ICT characteristics. The new emission band, which is gradually red-shifted with pressure, originated from the ICT state.[64] This is also evident from the change in UV-VIS absorption spectra of **PySS** with increasing pressure (Fig. S19, ESI†). We also performed the Raman spectra of **PySS** with different amounts of hydraulic pressure (Fig. S27, ESI†), and there was no significant change found in the spectra; it was only observed that the peak intensity reduced at higher pressure. This means that there might be a possibility that at high pressure the intermolecular distance decreases, thus the molecules approach

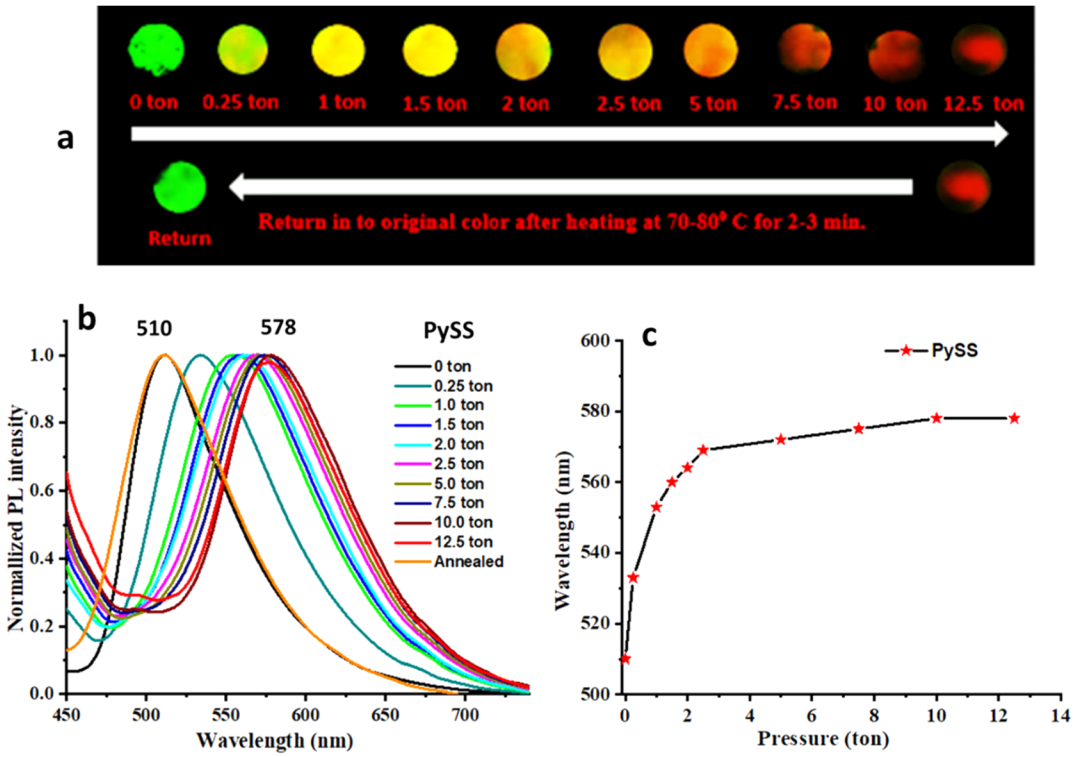

Fig. 6 PL properties of **PySS** under different amounts of hydraulic pressure. (a) Emission images of **PySS** taken under UV excitation (365 nm) with increasing pressure and after releasing pressure; (b) normalized PL spectra of **PySS** at different amounts of pressure; (c) the plot showing the change in wavelength at different amounts of pressure.

closer upon compression leading to the π–π stacking interactions.[65] The FESEM images of both samples were recorded (Fig. S28, ESI†). The pristine form shows a rod and sheet-type morphology, and after applying a shearing force (ground form) non-uniform micro-ranged particles formed.

The mechanism behind the gradual change of emission color of **PySS** and **PySP** was investigated by applying compressive force. The packing diagram shows that two molecules are arranged in an anti-parallel orientation, forming a molecular pair with two interactions. This molecular pair further extended axially to a long-range one-dimensional chain-type arrangement. In the case of **PySS**, two molecules interacted through π-electrons of one carbon of the pyrene ring with the H of the thiophene ring (π(C27)···H1 = 2.796 Å) forming a molecular pair and it is further extended through H-bonded interaction (H26···O1 = 2.685 Å) to another molecular pair in a one-dimensional fashion. These molecular pairs are extended in one direction linearly and form a one-dimensional chain (Fig. 7a). Each of these one-dimensional chains interacts sidewise with the neighboring parallel and similar chain held with a total of four different interactions (Fig. 7b and Table S4, ESI†). Similarly, for the case of **PySP** (Fig. 8a), two molecules connected through C–H···π interaction (C26···H11 = 2.843 Å) and further extended linearly through the hydrogen of pyrene with the pyridine ring hydrogen (H3···H20 = 2.329 Å) forming a one-dimensional chain. This one-dimensional chain is further connected sidewise to the neighboring parallel chain through a total of three different interactions (Fig. 8b and Table S4, ESI†). From the crystal packing, it was observed that planar pyrene rings are separated with twisted thiophene and pyridine. Thus, it is presumed that by the application of compressive force the rigid twisted thiophene ring becomes planar and comes closer forming a molecular pair of pyrenes (see packing in Fig. S22, ESI†). A similar kind of molecular packing was observed for the AIE active salicylaldehyde-based Schiff base reported by our group,[47] which was also given reversible MFC properties under hydraulic pressure.

It is noted that in both the cases (**PySS** and **PySP**), the MFC properties were reversible under the application of shearing force and hydraulic pressure, which is contradictory to the earlier report of our group,[47] where the emission change by shearing force is not reversible. It was observed that in the case of shearing force, the emission properties are reversible within 1.0 h at ambient conditions. Surprisingly, the reversibility process takes longer time for the hydraulic press one (~24 h at ambient conditions). From the crystal packing, it is speculated that molecular pairs that help to form a regular arrangement of crystals will mostly be intact under shearing force. So, after releasing pressure the ground sample recovers its original emission. On the other hand, it was observed from the crystal packing that flat pyrene rings are arranged in such a way that with the application of compressive force (hydraulic press), planarization of the molecule increases, and thus the molecules become close to each other. This enhances the π–π stacking

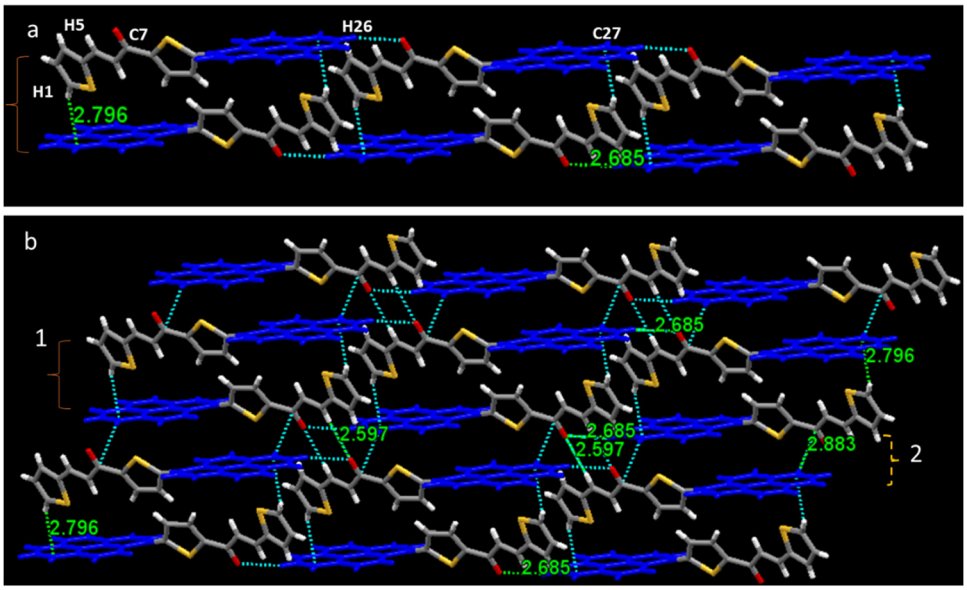

Fig. 7 (a) Crystal packing of **PySS** showing molecule faces opposite to each other and extended in one direction and (b) crystal packing of **PySS** with intermolecular interactions between molecules.

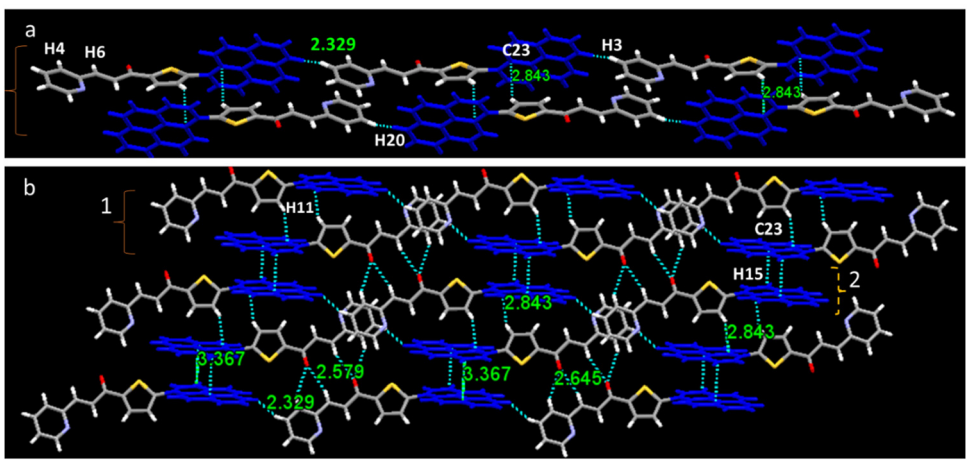

Fig. 8 (a) Crystal packing of **PySS** showing interactions and short contacts between molecules and (b) crystal packing of **PySP** with intermolecular interactions between molecules.

interactions that ultimately result in a decrease in emission intensity with red-shifting.[43] Upon releasing the pressure, the intermolecular interactions get loosened, and thus the molecules return to their original position (green emission) slowly.

Feasibility study for the application of PySS and PySP for reversible data storage and VOCs

The reversible color-switching features of **PySS** and **PySP** offer a promising reusable and secured platform for anticounterfeiting applications. An economical paper strip-based device is fabricated by dispersing green emitting solid (**PySS**) on a Whatman filter paper, demonstrated in security writing and piezo patterning applications.[60] A needle spatula was used to write on the paper, and after writing the emission color changed from green to yellow (Fig. 9), which happens because of the stress arising from the MFC property. This phenomenon is reversible; after heating/fuming with MeOH, its emission color returned to its original form (green emission). It may be useful in security data storage applications. Interestingly, if we expose the DCM vapor to the paper film of **PySS**, it converts its emission color from green to yellow. On the probe-impregnated filter paper, the letter R was written with DCM and exposed to MeOH vapor; its emission color returned to its original emission (Fig. 9b). Similarly, **PySP** was coated on filter paper and used for re-writable paper and DCM spot sensors (Fig. S29, ESI†). This way, reversible MFC properties of the probe could be useful for rewritable paper and sensing of volatile organic compounds.

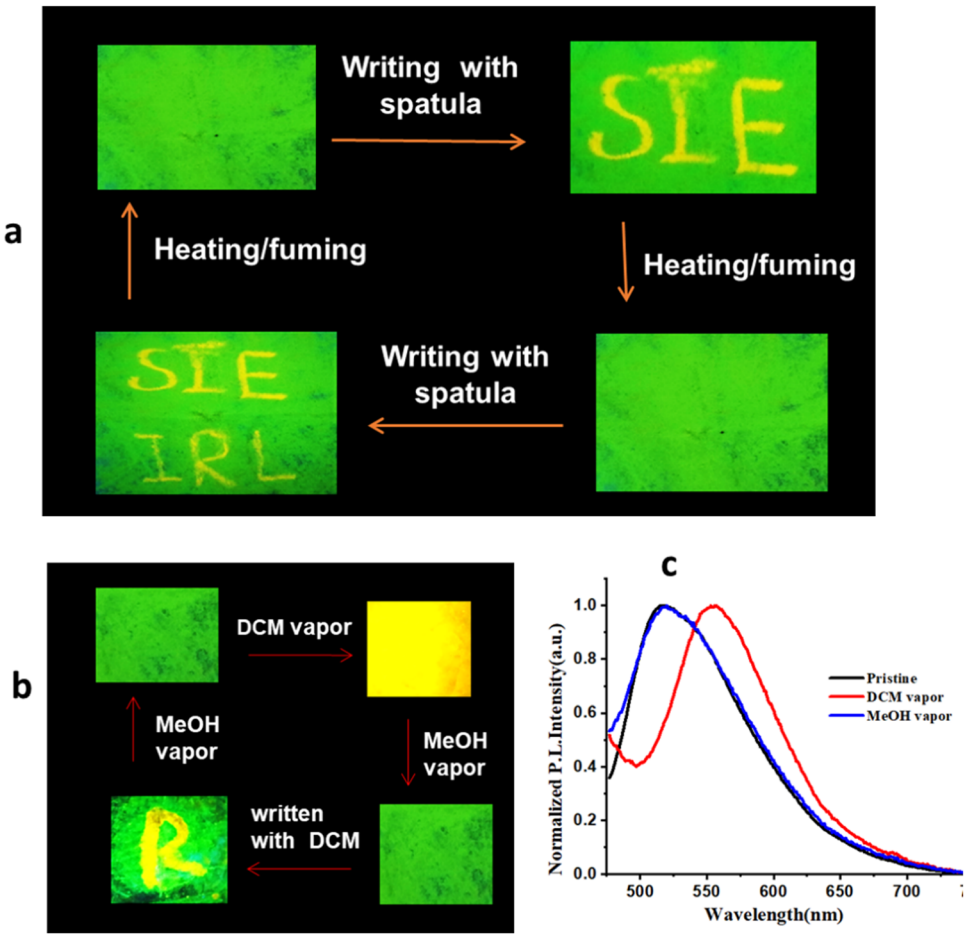

Fig. 9 **PySS** is used for stress sensing and VOC sensors. (a) Images of **PySS** taken under excitation of UV light (375 nm); the initially green emission after writing with a spatula (written S I E) converted to yellow, and then heating (70–80 °C)/fuming with methanol returned it to the original state and the process could be repeated. (b) Images of **PySS** under UV (365 nm) excitation (green emission); after exposing to DCM vapor, yellow emission is observed, and then after methanol fumigation, it returns to the original (green) emission. (c) Mormalized PL spectra of **PySS**, black line initial emission, red line after DCM vapor exposer and blue line is return with MeOH vapor.

Conclusion

Pyrene-thiophene based high-contrast MFC materials (**PySS** and **PySP**), which are sensitive to both grinding and compressive force, have been strategically designed and synthesized. Furthermore, **PySS** and **PySP** were found to be responsive towards solvent polarity with a large Stokes shift (147 nm and 130 nm). Interestingly, **PySS** gives a tunable color change by slowly increasing the hydraulic force (compressive), which is reversible in nature. By solvent fumigation or heating, it could be reconverted into its original emission within 2 min for grinding and compressive force. The sensitive MFC properties have been employed to demonstrate security ink and data storage devices. The packing diagram of both compounds showed a head–tail pair followed by a linear chain axially and it leads to a sheet with a layer-based structure. The present study and the earlier studies[47] support that the following arrangement of the molecules in the crystal would be responsible for the resulting highly sensitive and tunable emission by compressive force. Certainly, this work will inspire the finer designing of compounds that will result in more precise and controllable reversible tunable emission color.

Ethics statement

There are no ethical issues in this work.

Data availability

All the data are available in the ESI† and raw data will be made available to readers when requested.

Conflicts of interest

The authors have no conflict of interest to declare.

Acknowledgements

RPB gratefully acknowledges Birla Institute of Technology and Science (BITS) Pilani, Pilani campus, Rajasthan (India) for the fellowship. VV thanks CSIR for SRF. The 'UGC-sponsored Special Assistance Program (F.540/14/DRS/2007, SAP-I)' and DST-FIST programs in the chemistry department are acknowledged for instrumental support. We are also thankful to the Department of Physics, BITS Pilani, Pilani campus for the X-ray powder diffraction facility sponsored by DST-FIST. We are obliged to the central instrument facility of BITS Pilani for NMR, TGA, DSC and other instrumentation facilities. ARC and VV thank IISER Mohali for the ''XtaLab mini'' single crystal X-ray facility at the Department of Chemical Sciences, IISER Mohali.

References

1 V. Kachwal and I. R. Laskar, Mechanofluorochromism with Aggregation-Induced Emission (AIE) Characteristics: A Perspective Applying Isotropic and Anisotropic Force, *Top. Curr. Chem.*, 2021, **379**(4), 28.

2 Y. Hong, L. Meng, S. Chen, C. W. T. Leung, L.-T. Da, M. Faisal, D.-A. Silva, J. Liu, J. W. Y. Lam and X. Huang, Monitoring and inhibition of insulin fibrillation by a small organic fluorogen with aggregation-induced emission characteristics, *J. Am. Chem. Soc.*, 2012, **134**(3), 1680–1689.

3 M. Chen, R. Chen, Y. Shi, J. Wang, Y. Cheng, Y. Li, X. Gao, Y. Yan, J. Z. Sun and A. Qin, Malonitrile-functionalized tetraphenylpyrazine: aggregation-induced emission, ratiometric detection of hydrogen sulfide, and mechanochromism, *Adv. Funct. Mater.*, 2018, **28**(6), 1704689.

4 H. Wang, X. Ji, Z. A. Page and J. L. Sessler, Fluorescent materials-based information storage, *Mater. Chem. Front.*, 2020, **4**(4), 1024–1039.

5 A. Li, Z. Ma, J. Wu, P. Li, H. Wang, Y. Geng, S. Xu, B. Yang, H. Zhang and H. Cui, Pressure-Induced Wide-Range Reversible Emission Shift of Triphenylamine-Substituted Anthracene via Hybridized Local and Charge Transfer (HLCT) Excited State, *Adv. Opt. Mater.*, 2018, **6**(3), 1700647.

6 Y. Sun, Z. Lei and H. Ma, Twisted aggregation-induced emission luminogens (AIEgens) contribute to mechanochromism materials: a review, *J. Mater. Chem. C*, 2022, **10**(40), 14834–14867.

7 C. Xing, Z. Qi, B. Zhou, D. Yan and W. H. Fang, Solid-State Photochemical Cascade Process Boosting Smart Ultralong Room-Temperature Phosphorescence in Bismuth Halides, *Angew. Chem.*, 2024, **136**(21), e202402634.

8 C. Bustamante, L. Alexander, K. Maciuba and C. M. Kaiser, Single-Molecule Studies of Protein Folding with Optical Tweezers, *Annu. Rev. Biochem.*, 2020, **89**, 443–470.

9 Y. Hong, J. W. Lam and B. Z. Tang, Aggregation-induced emission, *Chem. Soc. Rev.*, 2011, **40**(11), 5361–5388.

10 Z. Zhao, B. He and B. Z. Tang, Aggregation-induced emission of siloles, *Chem. Sci.*, 2015, **6**(10), 5347–5365.

11 B. Z. Tang, X. Zhan, G. Yu, P. P. S. Lee, Y. Liu and D. Zhu, Efficient blue emission from siloles, *J. Mater. Chem.*, 2001, **11**(12), 2974–2978.

12 W. Z. Yuan, Y. Tan, Y. Gong, P. Lu, J. W. Y. Lam, X. Y. Shen, C. Feng, H. H. Y. Sung, Y. Lu, I. D. Williams, J. Z. Sun, Y. Zhang and B. Z. Tang, Synergy between Twisted Conformation and Effective Intermolecular Interactions: Strategy for Efficient Mechanochromic Luminogens with High Contrast, *Adv. Mater.*, 2013, **25**(20), 2837–2843.

13 Y. Xiong, J. Huang, Y. Liu, B. Xiao, B. Xu, Z. Zhao and B. Z. Tang, High-contrast luminescence dependent on polymorphism and mechanochromism of AIE-active (4-(phenothiazin-10-yl)phenyl)(pyren-1-yl)methanone, *J. Mater. Chem. C*, 2020, **8**(7), 2460–2466.

14 C. Li, X. Luo, W. Zhao, C. Li, Z. Liu, Z. Bo, Y. Dong, Y. Q. Dong and B. Z. Tang, Switching the emission of tetrakis(4-methoxyphenyl)ethylene among three colors in the solid state, *New J. Chem.*, 2013, **37**(6), 1696–1699.

15 P. Galer, R. C. Korošec, M. Vidmar and B. Šket, Crystal Structures and Emission Properties of the BF2 Complex 1-Phenyl-3-(3,5-dimethoxyphenyl)-propane-1,3-dione: Multiple Chromisms, Aggregation- or Crystallization-Induced Emission, and the Self-Assembly Effect, *J. Am. Chem. Soc.*, 2014, **136**(20), 7383–7394.

16 M. Chakraborty and M. Chakravarty, Variation in solvato-, AIE-and mechano-fluorochromic behavior for furanyl and thiophenyl-substituted anthranyl π-conjugates: the role of tiny flanking donor groups, *Mater. Adv.*, 2021, **2**(19), 6418–6427.

17 Y. Dong, B. Xu, J. Zhang, X. Tan, L. Wang, J. Chen, H. Lv, S. Wen, B. Li, L. Ye, B. Zou and W. Tian, Piezochromic Luminescence Based on the Molecular Aggregation of 9,10-Bis((E)-2-(pyrid-2-yl)vinyl)anthracene, *Angew. Chem., Int. Ed.*, 2012, **51**(43), 10782–10785.

18 J. Li, S. Yuan, J.-S. Qin, L. Huang, R. Bose, J. Pang, P. Zhang, Z. Xiao, K. Tan, A. V. Malko, T. Cagin and H.-C. Zhou, Fluorescence Enhancement in the Solid State by Isolating Perylene Fluorophores in Metal–Organic Frameworks, *ACS Appl. Mater. Interfaces*, 2020, **12**(23), 26727–26732.

19 X. Li, Q. Gao, J. Wang, Y. Chen, Z.-H. Chen, H.-S. Xu, W. Tang, K. Leng, G.-H. Ning, J. Wu, Q.-H. Xu, S. Y. Quek, Y. Lu and K. P. Loh, Tuneable near white-emissive two-dimensional covalent organic frameworks, *Nat. Commun.*, 2018, **9**(1), 2335.

20 X. Wang, J. Zhang, X. Mao, Y. Liu, R. Li, J. Bai, J. Zhang, C. Redshaw, X. Feng and B. Z. Tang, Intermolecular Hydrogen-Bond-Assisted Solid-State Dual-Emission Molecules with Mechanical Force-Induced Enhanced Emission, *J. Org. Chem.*, 2022, **87**(13), 8503–8514.

21 C. Liu, G. Xiao, M. Yang, B. Zou, Z.-L. Zhang and D.-W. Pang, Mechanofluorochromic Carbon Nanodots: Controllable Pressure-Triggered Blue- and Red-Shifted Photoluminescence, *Angew. Chem., Int. Ed.*, 2018, **57**(7), 1893–1897.

22 Y.-J. Ma, X. Fang, G. Xiao and D. Yan, Dynamic Manipulating Space-Resolved Persistent Luminescence in Core–Shell MOFs Heterostructures via Reversible Photochromism, *Angew. Chem., Int. Ed.*, 2022, **61**(2), e202114100.

23 G. Xiao, B. Zhou, X. Fang and D. Yan, Room-Temperature Phosphorescent Organic-Doped Inorganic Frameworks Showing Wide-Range and Multicolor Long-Persistent Luminescence, *Research*, 2021, **2021**, 9862327.
24 J. Mei, Y. Hong, J. W. Y. Lam, A. Qin, Y. Tang and B. Z. Tang, Aggregation-Induced Emission: The Whole Is More Brilliant than the Parts, *Adv. Mater.*, 2014, **26**(31), 5429–5479.
25 B. Valeur, Molecular Fluorescence, *Encyclopedia of Applied Physics*, 2009, pp. 477–531.
26 J. Xiong, K. Wang, Z. Yao, B. Zou, J. Xu and X.-H. Bu, Multi-Stimuli-Responsive Fluorescence Switching from a Pyridine-Functionalized Tetraphenylethene AIEgen, *ACS Appl. Mater. Interfaces*, 2018, **10**(6), 5819–5827.
27 W. Yang, C. Li, M. Zhang, W. Zhou, R. Xue, H. Liu and Y. Li, Aggregation-induced emission and intermolecular charge transfer effect in triphenylamine fluorophores containing diphenylhydrazone structures, *Phys. Chem. Chem. Phys.*, 2016, **18**(40), 28052–28060.
28 J. Jia and H. Zhao, Structure-dependent reversible mechanochromism of D-π-A triphenylamine derivatives, *Tetrahedron Lett.*, 2019, **60**(3), 252–259.
29 M. Fang, J. Yang, Q. Liao, Y. Gong, Z. Xie, Z. Chi, Q. Peng, Q. Li and Z. Li, Triphenylamine derivatives: different molecular packing and the corresponding mechanoluminescent or mechanochromism property, *J. Mater. Chem. C*, 2017, **5**(38), 9879–9885.
30 M. Yoshizawa and J. K. Klosterman, Molecular architectures of multi-anthracene assemblies, *Chem. Soc. Rev.*, 2014, **43**(6), 1885–1898.
31 B. Sun, X. Yang, L. Ma, C. Niu, F. Wang, N. Na, J. Wen and J. Ouyang, Design and Application of Anthracene Derivative with Aggregation-Induced Emission Charateristics for Visualization and Monitoring of Erythropoietin Unfolding, *Langmuir*, 2013, **29**(6), 1956–1962.
32 J. Zhao, Z. Chi, Z. Yang, Z. Mao, Y. Zhang, E. Ubba and Z. Chi, Recent progress in the mechanofluorochromism of distyrylanthracene derivatives with aggregation-induced emission, *Mater. Chem. Front.*, 2018, **2**(9), 1595–1608.
33 Y. Gu, K. Wang, Y. Dai, G. Xiao, Y. Ma, Y. Qiao and B. Zou, Pressure-Induced Emission Enhancement of Carbazole: The Restriction of Intramolecular Vibration, *J. Phys. Chem. Lett.*, 2017, **8**(17), 4191–4196.
34 X. Mei, K. Wei, G. Wen, Z. Liu, Z. Lin, Z. Zhou, L. Huang, E. Yang and Q. Ling, Carbazole-based diphenyl maleimides: Multi-functional smart fluorescent materials for data process and sensing for pressure, explosive and pH, *Dyes Pigm.*, 2016, **133**, 345–353.
35 Y. Takeda, H. Mizuno, Y. Okada, M. Okazaki, S. Minakata, T. Penfold and G. Fukuhara, Hydrostatic Pressure-Controlled Ratiometric Luminescence Responses of a Dibenzo[a,j]phenazine-Cored Mechanoluminophore, *ChemPhotoChem*, 2019, **3**(12), 1203–1211.
36 Y. Yang, A. Li, Z. Ma, J. Liu, W. Xu, Z. Ma and X. Jia, Dibenzo[a,c]phenazine-phenothiazine dyad: AIEE, polymorphism, distinctive mechanochromism, high sensitivity to pressure, *Dyes Pigm.*, 2020, **181**, 108575.
37 S. Ghosh, H. Bhambri, A. K. Singh, S. K. Mandal, L. Roy and P. S. Addy, A convenient route to a vinylogous dicyano aryl based AIEgen with switchable mechanochromic luminescence properties, *Chem. Commun.*, 2023, **59**(30), 4463–4466.
38 X. Meng, G. Qi, X. Li, Z. Wang, K. Wang, B. Zou and Y. Ma, Spiropyran-based multi-colored switching tuned by pressure and mechanical grinding, *J. Mater. Chem. C*, 2016, **4**(32), 7584–7588.
39 Y. Xu, K. Wang, Y. Zhang, Z. Xie, B. Zou and Y. Ma, Fluorescence mutation and structural evolution of a π-conjugated molecular crystal during phase transition, *J. Mater. Chem. C*, 2016, **4**(6), 1257–1262.
40 J. M. Robertson and J. White, 72. The crystal structure of pyrene. A quantitative X-ray investigation, *J. Chem. Soc.*, 1947, 358–368.
41 M. Fang, J. Yang and Z. Li, Light emission of organic luminogens: Generation, mechanism and application, *Prog. Mater. Sci.*, 2022, **125**, 100914.
42 E. V. Varghese, C.-Y. Yao and C.-H. Chen, Investigation of Mechanochromic Luminescence of Pyrene-based Aggregation-Induced Emission Luminogens: Correlation between Molecular Packing and Luminescence Behavior, *Chem. – Asian J.*, 2024, **19**(1), e202300910.
43 Y. Xiong, J. Huang, Y. Liu, B. Xiao, B. Xu, Z. Zhao and B. Z. Tang, High-contrast luminescence dependent on polymorphism and mechanochromism of AIE-active (4-(phenothiazin-10-yl)phenyl)(pyren-1-yl)methanone, *J. Mater. Chem. C*, 2020, **8**(7), 2460–2466.
44 X. Feng, X. Wang, C. Redshaw and B. Z. Tang, Aggregation behaviour of pyrene-based luminescent materials, from molecular design and optical properties to application, *Chem. Soc. Rev.*, 2023, **52**, 6715–6753.
45 M. M. Islam, Z. Hu, Q. Wang, C. Redshaw and X. Feng, Pyrene-based aggregation-induced emission luminogens and their applications, *Mater. Chem. Front.*, 2019, **3**(5), 762–781.
46 P. Sonar, M. S. Soh, Y. H. Cheng, J. T. Henssler and A. Sellinger, 1,3,6,8-tetrasubstituted pyrenes: solution-processable materials for application in organic electronics, *Org. Lett.*, 2010, **12**(15), 3292–3295.
47 S. S. Pasha, H. R. Yadav, A. R. Choudhury and I. R. Laskar, Synthesis of an aggregation-induced emission (AIE) active salicylaldehyde based Schiff base: study of mechanoluminescence and sensitive Zn(II) sensing, *J. Mater. Chem. C*, 2017, **5**(37), 9651–9658.
48 R. P. Bhatta, V. Kachwal, C. Climent, M. Joshi, P. Alemany, A. R. Choudhury and I. R. Laskar, Tunable emission in the visible range from a single organic fluorophore through time-controlled morphological evolution, *J. Mater. Chem. C*, 2023, **11**(33), 11399–11408.
49 M. J. Frisch, G. W. Trucks, H. B. Schlegel, G. E. Scuseria, M. A. Robb, J. R. Cheeseman, G. Scalmani, V. Barone, B. Mennucci, G. A. Petersson, *et al.*, *Gaussian 09, Revision A.01*, Gaussian. Inc., Wallingford CT, 2009, vol. 121, pp. 150–166.
50 W. J. Hehre, R. Ditchfield and J. A. Pople, Self—consistent molecular orbital methods. XII. Further extensions of

Gaussian—type basis sets for use in molecular orbital studies of organic molecules, *J. Chem. Phys.*, 1972, **56**(5), 2257–2261.

51 M. Frisch, G. Trucks, H. B. Schlegel, G. Scuseria, M. Robb, J. Cheeseman, G. Scalmani, V. Barone, G. Petersson and H. Nakatsuji, *Gaussian 16*, Gaussian, Inc., Wallingford, CT, 2016.

52 J.-D. Chai and M. Head-Gordon, Long-range corrected hybrid density functionals with damped atom–atom dispersion corrections, *Phys. Chem. Chem. Phys.*, 2008, **10**(44), 6615–6620.

53 Y.-B. Gong, P. Zhang, Y.-R. Gu, J.-Q. Wang, M.-M. Han, C. Chen, X.-J. Zhan, Z.-L. Xie, B. Zou, Q. Peng, Z.-G. Chi and Z. Li, The Influence of Molecular Packing on the Emissive Behavior of Pyrene Derivatives: Mechanoluminescence and Mechanochromism, *Adv. Opt. Mater.*, 2018, **6**(16), 1800198.

54 E. V. Varghese, C. Y. Yao and C. H. Chen, Investigation of Mechanochromic Luminescence of Pyrene-based Aggregation-Induced Emission Luminogens: Correlation between Molecular Packing and Luminescence Behavior, *Chem. – Asian J.*, 2024, **19**(1), e202300910.

55 S.-W. Yang, A. Elangovan, K.-C. Hwang and T.-I. Ho, Electronic polarization reversal and excited state intramolecular charge transfer in donor/acceptor ethynylpyrenes, *J. Phys. Chem. B*, 2005, **109**(35), 16628–16635.

56 A. D'Aléo, A. Karapetyan, V. Heresanu, M. Giorgi and F. Fages, Tuning solid-state emission properties of pyrene-containing chalcone derivatives, *Tetrahedron*, 2015, **71**(15), 2255–2259.

57 Z. Huang, F. Tang, F. He, L. Kong, J. Huang, J. Yang and A. Ding, Pyrene and triphenylamine substituted cyanostyrene and cyanostilbene derivatives with dual-state emission for high-contrast mechanofluorochromism and cell imaging, *Org. Chem. Front.*, 2022, **9**(19), 5118–5124.

58 Z. Zhao, S. Chen, J. W. Y. Lam, Z. Wang, P. Lu, F. Mahtab, H. H. Y. Sung, I. D. Williams, Y. Ma, H. S. Kwok and B. Z. Tang, Pyrene-substituted ethenes: aggregation-enhanced excimer emission and highly efficient electroluminescence, *J. Mater. Chem.*, 2011, **21**(20), 7210–7216.

59 Y. Kim, J. Bouffard, S. E. Kooi and T. M. Swager, Highly Emissive Conjugated Polymer Excimers, *J. Am. Chem. Soc.*, 2005, **127**(39), 13726–13731.

60 M. Chakraborty and M. Chakravarty, Varied optical features and mechanofluorochromism in dicyanovinyl-vs. cyanoacrylic-acid-linked twisted π-conjugates: A potential reusable platform for security applications, *Mater. Today Chem.*, 2024, **35**, 101836.

61 G. Niu, X. Zheng, Z. Zhao, H. Zhang, J. Wang, X. He, Y. Chen, X. Shi, C. Ma, R. T. K. Kwok, J. W. Y. Lam, H. H. Y. Sung, I. D. Williams, K. S. Wong, P. Wang and B. Z. Tang, Functionalized Acrylonitriles with Aggregation-Induced Emission: Structure Tuning by Simple Reaction-Condition Variation, Efficient Red Emission, and Two-Photon Bioimaging, *J. Am. Chem. Soc.*, 2019, **141**(38), 15111–15120.

62 P. S. Hariharan, V. K. Prasad, S. Nandi, A. Anoop, D. Moon and S. P. Anthony, Molecular engineering of triphenylamine based aggregation enhanced emissive fluorophore: structure-dependent mechanochromism and self-reversible fluorescence switching, *Cryst. Growth Des.*, 2017, **17**(1), 146–155.

63 X. Wang, Q. Liu, H. Yan, Z. Liu, M. Yao, Q. Zhang, S. Gong and W. He, Piezochromic luminescence behaviors of two new benzothiazole–enamido boron difluoride complexes: intra- and inter-molecular effects induced by hydrostatic compression, *Chem. Commun.*, 2015, **51**(35), 7497–7500.

64 Q. Qi, J. Qian, X. Tan, J. Zhang, L. Wang, B. Xu, B. Zou and W. Tian, Remarkable Turn-On and Color-Tuned Piezochromic Luminescence: Mechanically Switching Intramolecular Charge Transfer in Molecular Crystals, *Adv. Funct. Mater.*, 2015, **25**(26), 4005–4010.

65 A. Li, P. Li, Y. Geng, S. Xu, H. Zhang, H. Cui and W. Xu, Investigation of supramolecular interaction in 4,4′-bipyridine crystal by hydrostatic pressure spectroscopies, *Spectrochim. Acta, Part A*, 2018, **202**, 70–75.

